1. Introduction

In recent years, there has been a great deal of interest in facilitating space access through the design of efficient and reliable space transportation systems. For the design of thermal protection systems, rocket propulsion systems and hypersonic air-breathing propulsion systems, the proper prediction of thermal and structural loads is a crucial task. Although experimental methods provide an essential means for the validation of simulation results and the verification of entire subsystems, not all flow field quantities of interest are accessible to measurements and tight budgets may prohibit extensive and costly experimental campaigns. As a remedy, accurate and easy to handle tools are urgently needed throughout the entire design phase.

External and internal hypersonic high-enthalpy flows are characterized by a wide range of physically relevant phenomena on various time and length scales.[4] This includes shock patterns spread over wide areas of the flow field, boundary layers, entropy layers as well as the interaction of all of these flow phenomena, potentially in an unsteady flow field. Within shock and boundary layers, internal energy modes of the gas molecules are excited and chemical reactions are triggered. Thermochemical relaxation processes may occur on small length scales, but may have an impact on the entire flow field as the gas properties may be significantly and rapidly altered.

The proper resolution of these multiphysics phenomena at various length scales is a challenging task for every flow solver, both in terms of physical modeling as well as the applied numerical methods. Grid quality has a significant influence on the solution and a properly designed grid is a necessity for any flow simulation. Capturing thermochemical nonequilibrium effects in shock and boundary layers requires a locally high grid resolution. At the same time, the high computational costs of thermochemical nonequilibrium models prohibit the use of overly or inefficiently refined grids. However, the manual design of high-quality grids is cumbersome. In order to keep the number of grid cells and the resulting computational costs low, the user must have an a-priori knowledge of the flow field solution to refine the grid accordingly. This requires labor-intensive manual work on the mesh, especially when the grid needs to be readjusted several times as a part of an iterative solution process in cases where no a-priori knowledge of the solution is available.

A possible remedy to this is the use of grid adaptation methods. The automatic detection of flow features significantly reduces manual work on the grid. For steady-state simulations, the solution process may be started on a coarse base discretization, which is successively refined during the solution process. The computational effort is

significantly reduced through a grid that is tailored to the flow field solution. In addition, the solution on a given grid level may be used as an initial guess for the subsequent grid level. This further reduces the time to establish and relocate flow features.

Several approaches[118,12] exist to conduct a local grid adaptation. p-adaptation locally changes the order of the numerical scheme. r-adaptation globally re-meshes a grid with a given and constant number of cells by moving existing cell nodes into areas where a higher resolution is required. This approach greatly facilitates data management as the overall number and the logical connection of the grid cells remains constant. Another, more flexible approach is h-adaptation, where the cells are locally subdivided and enriched by additional cells. At the expense of hanging nodes at the interfaces between different refinement levels, major h-refinement methods result in a tree-like sequence of nested grids with a potentially high local resolution.

Suitable criteria are required for driving the adaptation mechanism. This is a crucial and challenging task, especially in hypersonic flow fields where flow features are found on various length scales. Local indicators[14] are frequently taken into account for driving the adaptation mechanism. In general, the adaptation criterion may be based on[118] (a) solution features or the reconstruction of values or gradients, (b) adjoint methods, or (c) truncation errors and residuals.

Adaptive Mesh Refinement (AMR) is a grid adaptation method which is frequently used for hypersonic flows. It relies on a sequence of nested grid patches which are superimposed on a structured[12] or unstructured coarse grid. Local error estimators are used to drive the adaptation mechanism. For instance, Kirk[70] employs a gradient or flux-jump error indicator combined with a problem-dependent selection criterion to identify relevant areas for refinement. In general, AMR methods involve a considerable effort in programming and data management[28] and the local error estimators and selection criteria need to be properly adjusted to the solved flow problem.

AMR is applied in various Computational Fluid Dynamics (CFD) solvers for the simulation of compressible high-speed flows. An example is the Adaptive Mesh Refinement framework AMROC.[38] The block-structured adaptive mesh refinement is capable of achieving grids with an *"extraordinary high local resolution"*, but with the restriction to simple domains[1] because of its patch-wise refinement strategy. AMROC can be coupled to various flow solvers based on time-explicit finite volume methods.[1] Deiterding[38] applied a finite volume scheme which is second order in space to simulate complex Mach reflection structures in reactive $H_2 - O_2 - Ar$ gas mixtures. Another example of an AMR-based CFD code is implemented by Kirk.[70] In his work, the finite element based CFD solver is applied to a large variety of complex flow configurations. This includes the simulation of an Edney type IV shock-shock interaction.

As a replacement to AMR, alternative grid adaptation methods are also applied to compressible high-speed flows. An example of this is the DLR TAU[123] code, which is based on unstructured hybrid grids. The grid adaptation employs an edge-based data structure where the edges may be subdivided to allow for a local grid refinement. Areas

which require grid refinement are identified with edge-indicator sensor functions. These indicators may use gradients or differences along the edge of any suitable flow variable. The TAU code may be applied to a variety of flow configurations, including compressible flows in thermochemical nonequilibrium of various gas mixtures.

An alternative to the discussed refinement methods is the use of multiresolution techniques.[100] The multiscale-based grid adaptation works directly on the solution variables of the flow solver without the need for additional local error estimators. The key idea[28,12] is to transform the arrays of cell average data with the help of multiscale techniques, similar to those applied for image compression, into a different format which reveals insight into the solution behavior.

Such a multiscale-based grid adaptation is incorporated into the QUADFLOW[14] solver, an integrated framework of finite-volume method flow solver, grid generation and grid adaptation module. QUADFLOW was specifically designed for the solution of the compressible Navier-Stokes equations with the aim to cover flow simulations from transonic to hypersonic speeds. The multiscale-based grid adaptation concept is an essential and unique feature of the QUADFLOW solver. As no knowledge on the refined grid areas is available prior to running the simulation, a generalized and highly-accurate description of the grid is needed at runtime. This is realized through the grid generation module, which is based on a sparse B-Spline representation of the grids. This allows for an accurate function evaluation at any given point. The flow solver was specifically designed to handle unstructured grids with a potentially large number of hanging nodes. The initial version of the QUADFLOW solver was released in 2003 with contributions from the principal authors Müller[100] (grid adaptation), Lamby[81] (grid generation) and Bramkamp[12] (flow solver). Over the last decade, various authors contributed to the development of the QUADFLOW solver, making it a powerful and versatile tool which was validated with and applied to a large number of applications.[77,102,10,15]

1.1. Objectives of this Thesis

The aim of this work is to develop a general CFD solver framework which allows new insights into hypersonic nonequilibrium flow fields by delivering highly-resolved simulation results in an efficient way.

The QUADFLOW solver is modified and extended by providing the necessary physical models and numerical methods for the simulation of arbitrary reaction models in thermochemical nonequilibrium. The original implementation of the thermochemical nonequilibrium models in the QUADFLOW solver are based on previous work by Klomfaß[71] and Kumar.[80] In his thesis, Klomfaß focused on the thermodynamic modeling of nonequilibrium flows and introduced correlated models for the computation of the energy exchange among vibrational energy modes. For the purpose of validation, he implemented these models for 5-species air into a research code. Later on, the resulting code formed the basis of the NSCTNG2[99] solver. Kumar incorporated these NSCTNG2

routines for 5-species air into the QUADFLOW solver and extended the existing code with additional thermal nonequilibrium models from the literature. Kumar considered also the 2-species nitrogen model in his simulations. However, in his implementation, it was only a subset of the existing 5-species model where unused quantities were computed, but neglected afterwards.

In the current work, the existing models and the implementation are generalized and implemented in an efficient way. This extension builds upon a generalization of the QUADFLOW solver for inviscid flows in chemical nonequilibrium which was subject to previous work.[136,135] The aim of the current work is to provide a general framework which can be used for the simulation of thermochemical nonequilibrium gas mixtures with an arbitrary number of species. This includes the possibility to use any number of temperatures for simulations in thermal nonequilibrium. The temperatures may be formed from various energy modes in a user-defined way. Tools required for the computation and data exchange of curve fit data of the thermodynamic and transport properties are implemented. This provides a most flexible implementation which can be easily extended and applied to a wide range of applications.

Apart from the need of an accurate modeling of thermochemical nonequilibrium effects, simulations of hypersonic flows require robust, efficient and accurate numerical methods. This requires further modifications of the QUADFLOW solver. The convergence rate of the flow solver is significantly increased in the present work by providing the necessary means for the use of implicit or explicit-implicit time integration methods. The Jacobians for the nonequilibrium viscous fluxes are derived and implemented. Necessary interfaces for the Jacobians of the thermochemical source terms are incorporated and the derivation of the Jacobians is illustrated at the example of the Millikan and White vibrational-translational energy exchange. In view of the shock-shock interaction configurations considered in the present work, the stability of the convergence process and the grid quality is improved through the use of newly implemented piecewise grid stretching functions. The implementation of a second order approximation of the wall temperature gradient significantly improves the accuracy of the wall heat flux rates. A logarithmic approximation of the temperature gradient is discussed as an alternative approach. All nonequilibrium modules of the QUADFLOW solver, which utilize multiple programming languages (C++, C, FORTRAN), are parallelized based on the Message Passing Interface (MPI) standard and tuned for running on large-scale High Performance Computing (HPC) clusters.

The resulting QUADFLOW solver allows to properly capture thermochemical nonequilibrium flow fields with a locally very high resolution combined with a high efficiency. The proper resolution of small-scale flow features provides the user with new insights into high-speed flow fields. This could not be realized with Kumar's implementation of the QUADFLOW solver. Apart from various test cases for the purpose of validation, the capabilities of the present QUADFLOW solver will be demonstrated with two pertinent application test cases in the present work. Excerpts of these works were previously

published as preprints of this thesis by Windisch, Reinartz and Müller.[138,137] The injection of cooling gases into a supersonic laminar boundary layer represents a typical low enthalpy configuration. The flexible handling of the injection boundary condition demonstrates the versatility and flexibility of the grid adaptation concept. The proper resolution of the boundary and cooling layer demonstrates the robustness of the applied numerical methods. The simulated Edney type IV and Edney type VII shock-shock interactions are a pertinent example of complex unsteady flow phenomena. Especially the high dependency of the Edney type IV interaction problem on the mesh quality is one of the reasons why shock-shock interactions are difficult to simulate. The simulation result demonstrates the abilities of the modified QUADFLOW solver to capture the inner flow field and the boundary layer of this complex configuration at the same time and with a high resolution. The results enhance the understanding of the mechanism of the unsteady jet movements and allow for a classification of the unsteady jet behavior. The discussion addresses the difficult problem of grid convergence and provides new insight into the numerics and physics of this important shock-shock interaction. Potential pitfalls of inadequate numerical methods are discussed. The less known Edney type VII interaction is simulated using the gas composition of the Martian atmosphere. Planned interplanetary missions to Mars have spurred the interest of the research community which is in need to find adequate simulation capabilities. The results presented in this work demonstrate that the Edney type VII interaction occurs in CO_2 dominated gas mixtures and provide new insight into the flow field structure and the jet unsteady movement.

1.2. Outline

Chapter 2 will give a more detailed introduction into the considered application cases. A literature review will provide the reader with the necessary theoretical background. The applied physical and mathematical models are the subject of Chapter 3. Emphasis is placed on the modification and extension of the models for the simulation of gas mixtures with an arbitrary number of species and internal temperatures. The multiscale-based grid adaptation and all relevant numerical methods of the flow solver are discussed in Chapter 4. Chapter 5 discusses the validation of sole modules of the modified flow solver. This includes (a) external tools for the generation of appropriate curve fit data for the thermodynamic and transport properties, (b) the finite-rate chemistry model, the (c) temporal relaxation and (d) combined temporal and spatial relaxation of the nonequilibrium source terms. The QUADFLOW solver as a whole is validated with two different configurations of hypersonic flow around a cylinder and a nozzle flow configuration in Chapter 6. The cooling gas injection and the shock-shock interaction as application test cases follow in Chapters 7 and 8, respectively. The work is concluded with a brief summary in Chapter 9.

2. Test Configurations and Literature Review

The modified QUADFLOW solver presented in this work is applied to simulate two test configurations: A cooling gas injection into a laminar supersonic boundary layer and a shock-shock interaction which, depending on the test gas, results in an Edney type IV or Edney type VII interaction. More details on the selected configurations are given in the following, along with the necessary theoretical background and a state of the art summary from a brief literature review.

2.1. Cooling Gas Injection

2.1.1. Motivation

The use of either passive or active cooling techniques is a major approach to lower the thermal impact of supersonic high-enthalpy flows on the surrounding structures. Passive techniques, such as cooling by radiation or ablation, are widely used for thermal protection systems in external aerodynamics. However, these techniques cannot be adjusted during flight to account for different flight phases and the corresponding heat fluxes. Accordingly, the whole system must be designed for the peak heat flux which could lead to inefficient designs with large safety margins during other flight phases. Internal flows in rocket propulsion systems and hypersonic air-breathing propulsion also require highly efficient cooling techniques. Operating conditions of these systems may change significantly during flight and the cooling system must be able to handle high heat loads over a longer period of time. This is why active cooling techniques are preferred for these kinds of systems.

Active cooling techniques allow for an adjustment to the current flight phase and are based on the injection of a coolant into the boundary layer. The coolant can be injected either by using porous media or through distinct openings in the surface. Porous media allow for a uniform injection over a larger area which leads to low temperature gradients along the surface even for low coolant mass flow rates. Injecting the coolant through slots or boreholes in the surface allows for thicker cooling films in local hot spots, such as the nose region of a reentry vehicle. Besides, there are less restrictions on the selection of the surface material.

2.1.2. Literature Review

Film cooling is frequently used for turbine blades, where air is injected into the turbulent flow field through a series of single boreholes. Apart from this pertinent application, basic research on film cooling with higher blowing ratios in incompressible, subsonic flow fields is widely found in the early literature. An overview of fundamental studies concerning film cooling is given by Goldstein.[49] Driven by the development of space transportation systems, supersonic flow fields came more and more into the focus of the research community in subsequent years. Major theoretical and empirical approaches from various researchers, describing the efficiency of film cooling for various flow conditions, are discussed by Heufer.[59] Heufer's primary focus is on the injection of air into laminar supersonic flow fields. In his work, a theoretical approach for predicting the cooling efficiency is derived[60] and supported by experimental and numerical studies. Keller and Kloker[69] numerically investigated the film cooling of air injected into air through one or two rows of staggered, discrete holes. Both modeled and fully simulated injection channels are applied in this study. The influence of modeled versus simulated injection is discussed by Gotzen et al.[34] for a single-slot injection. While air as a coolant simplifies the investigation of the injection mechanism, actual applications frequently use different cooling gases. Holden[64] conducted experiments to analyze film cooling efficiencies in turbulent hypersonic flows with shock interactions. A supersonic jet of helium was injected tangentially into the flow field. Holden demonstrates a larger cooling efficiency of the helium coolant than for a nitrogen coolant used in previous investigations. Both measurements can be correlated by complex input parameters which include Mach number, specific heats and molar weights of the coolants. Cheuret et al.[27] investigated transpiration cooling through a porous medium applying air, helium and hydrogen as a coolant. In case of hydrogen and helium, due to their larger specific heat capacities, the mass flow rate can be greatly reduced while achieving the same cooling efficiency as when using air.

2.1.3. Test Configuration

The slot injection of various cooling gases into a laminar supersonic boundary layer was recently investigated in experiments by Hombsch and Olivier.[65] An inclined flat plate mounted on a wedge model is investigated in a hypersonic shock tunnel to create a supersonic laminar boundary layer. Various coolants at ambient temperature are injected. The effect of these coolants (air, argon, helium, sulfur(VI)fluoride, carbon dioxide) on the wall heat fluxes and the corresponding cooling efficiencies are measured.

The experiments by Hombsch and Olivier[65] are computationally investigated in Chapter 7. The lower temperatures of this configuration allow for the use of a reduced and computationally less expensive model, in particular a frozen gas mixture of thermally perfect gases in thermal equilibrium. Combined with the grid adaptation concept, this test case demonstrates the efficiency and flexibility of the QUADFLOW solver.

2.2. Edney Type IV and Type VII Shock-Shock Interaction

2.2.1. Motivation

Shock-shock interactions are characterized by a wide range of physically relevant flow phenomena.[40] These are located throughout the entire flow field and make the manual design of grids rather cumbersome. A pertinent example is the Edney type IV interaction, see Figures 2.1 and 2.2. This configuration is the result of an incident shock wave which impinges on the bow shock in front of a blunt body. The Edney type IV interaction is frequently used in theoretical and experimental investigations as it leads to high aerothermal loads on the body surface. Shock interactions of this or related types are frequently found in engineering applications. Depending on the particular configuration, Edney type IV interactions may show unsteady behavior. Due to their high frequency, these unsteady mechanisms cannot be fully captured by experimental investigations. Highly-resolved CFD simulations are the only means to investigate such configurations.

The proper simulation and prediction of these shock interaction patterns is a crucial task. The structure of the incident oblique shock wave and the main shock must be properly captured in order to predict the deflection of the flow field and the resulting shock pattern. Strong shocks are formed at a certain distance ahead of the vehicle surface and spread out over a larger area. In addition, the boundary layer needs to be properly resolved in order to capture the wall heat flux and to predict the thermal loads on the vehicle surface. Both areas are connected by strong interaction patterns, which are difficult to predict in strength and location and are potentially unstable.[54] To account for the high-temperature flow field behind the shock pattern, the physical modeling of the numerical simulation must consider nonequilibrium effects. The excitation of the internal energy modes and the resulting dissociations are yet another flow feature, which requires a locally very high resolution. In addition, the inherent instability of the Edney type IV and other shock-shock interactions is a challenging task, especially when considering the potentially unstable solution behavior of numerical simulations in chemical and thermochemical nonequilibrium. However, especially for the analysis of the high-frequency unsteady solution mechanisms, which are not fully accessible to experimental investigations, CFD simulations are an important means to gain further insight into these kinds of shock-shock interactions.

2.2.2. Literature Review

Classification of Shock-Shock Interactions Shock-shock interactions have been widely discussed in the literature over the past decades. Referring to Sanderson,[121] the shock interference pattern depends on the strength and angle of the intersecting shocks, the geometry of the body around which the interference pattern is formed, the relative location of the impinging shock on the body and the gas properties, i.e., the ratio of specific

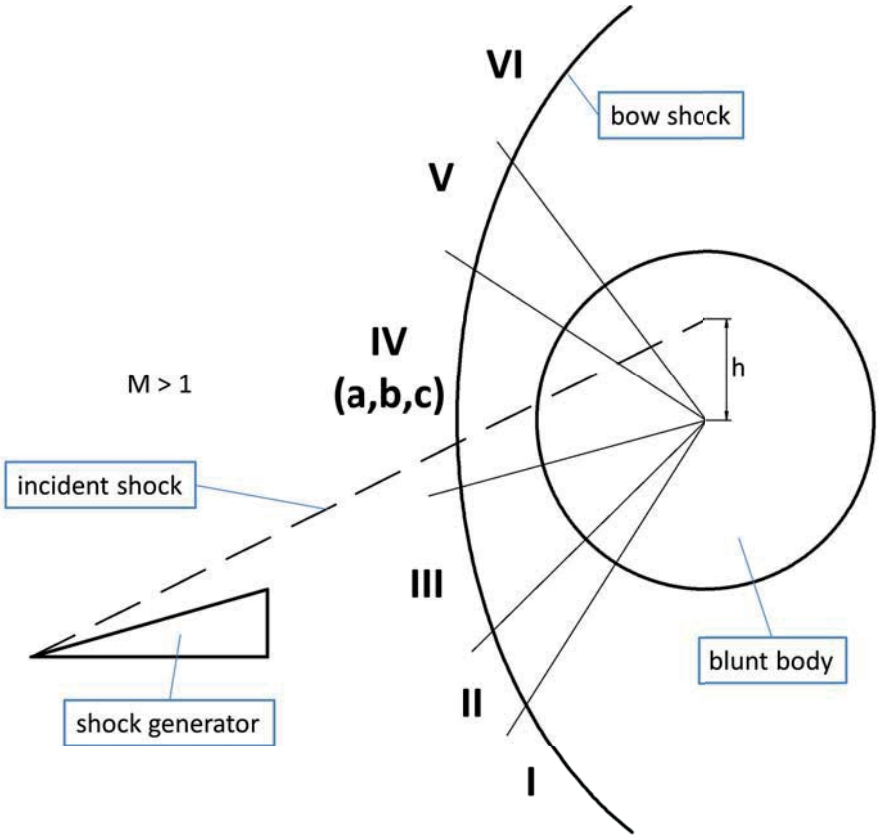

Figure 2.1.: Schematic drawing of the original Edney classification, after Grasso et al.[54]

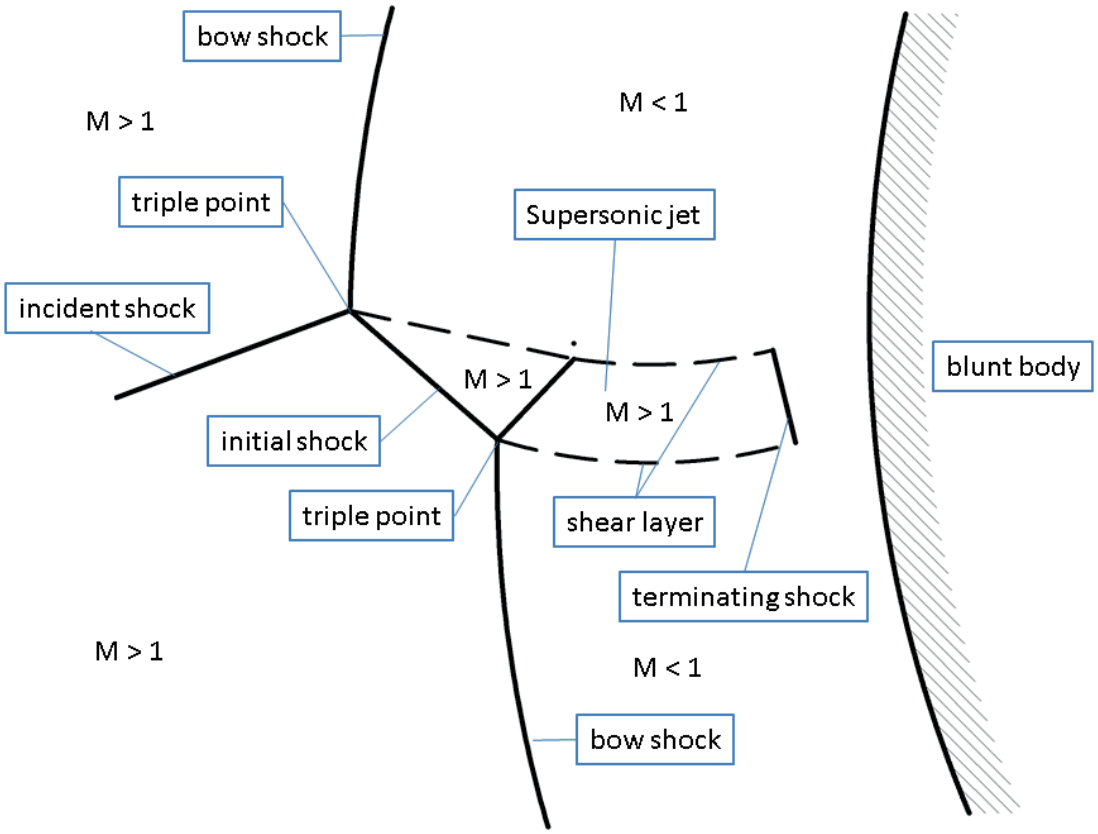

Figure 2.2.: Schematic drawing of the Edney type IV interaction, after Grasso et al.[54]

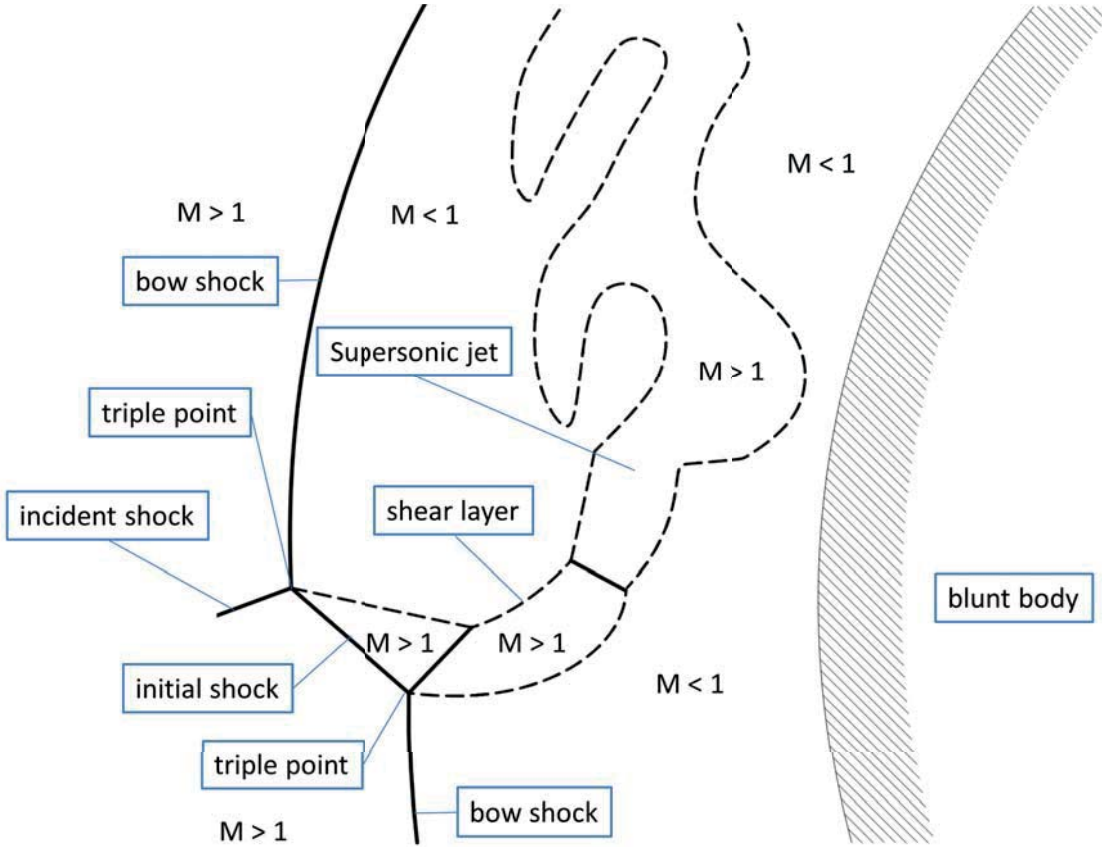

Figure 2.3.: Schematic drawing of the type VII interaction, after Yamamoto et al.[143]

heats. The most comprehensive classification of shock-shock interactions was carried out by Edney,[40] who experimentally and theoretically investigated the impingement of an oblique shock wave on a strong bow shock in front of a blunt body. Edney distinguished six shock-interaction patterns named as types I-VI. The particular type depends on the location of the impingement on the bow shock, compare Figure 2.1. The Edney type IV interaction is the most critical shock-shock interaction in terms of the aerothermal loads on the wall.[54,17] As a result, this type is most interesting for engineering applications. A detailed analysis of the front section of the shock interaction pattern was carried out for double-wedge geometries by Olejniczak et al.[105] A supersonic jet forms between two triple points and reaches into the subsonic region behind the bow shock, see Figure 2.2. The flow bends upwards by a combination of several expansion and compression waves. The wall impingement of the flow passing though the shock pattern of the jet and the terminating shock leads to high pressures and temperatures on the surface of the blunt body. This configuration exhibits an unstable behavior and is highly sensitive to the exact location h of the shock impingement. When the impinging shock wave is moved upward, the jet begins to bend upwards along the cylinder surface. This state is frequently characterized as a type IVa interaction,[54] which is an extension of the original Edney type I-VI classification. In addition to these widely accepted types, authors in the literature also identified shock-shock interactions in which the jet structure extends

away from the wall into the flow field. Yamamoto et al.[143] defined such an interaction as type VII, while other authors referred to similar configurations as types IVb,c. The type VII shock-shock interaction requires an impinging shock location similar to the types IVb,c as indicated in Figure 2.1. As Yamamoto et al. identified this interaction type only for a particular configuration, no information is available on the range of impingement locations leading to a type VII interaction. A schematic drawing of the particular configuration found by Yamamoto et al. is depicted in Figure 2.3.

Nonequilibrium effects In his work, Edney indicated the dependence of the shock-shock interaction pattern on the gas properties and related high-temperature effects. The influence of nonequilibrium effects has been computationally investigated by various authors.[16,70,43,143] While Edney[80,40] speculates in earlier investigations that high-temperature real gas effects will lead to increased heat flux rates, Kumar as well as other authors[121,43] demonstrated that increasing nonequilibrium effects decrease the actual heat flux rate. Following Brück[17] who investigated flows in thermochemical nonequilibrium, stronger chemical reactions lead to smaller shock stand-off distances which in turn reduces the size of the supersonic jet. Assuming a constant pressure difference across the shock train inside the supersonic jet, shorter jets are characterized by a stronger curvature and are less likely to impinge on the wall surface. This finding is confirmed by Yamamoto et al.[143] who found that the decreased shock stand-off distance leads to an increase in pressure in the area below the supersonic jet, which in turn leads to a stronger curved jet structure. They concluded from a study of nitrogen flow in thermochemical nonequilibrium that a strong decrease in the shock stand-off distance may even result in a change of the shock-shock interference type. For large values of the impingement shock location h, see Figure 2.1, a new type of shock-shock interference was experienced which involves a *"supersonic jet streaming toward the upper downstream without stagnating on the body"*. This is in contrast to the type IVa interaction in which case the supersonic jet still touches the wall surface. Yamamoto et al.[143] referred to this new interaction as type VII. The supersonic jet is characterized by a strong vorticity. The vibrational temperature and the resulting reaction rates within the jet structure are low. The details of this jet structure, which remain subject to further investigation and clear classification, are discussed in Section 8.4.

Grid Dependency The vast majority of the simulations of shock-shock interactions rely on the use of non-adaptive, mostly structured grids. The use of non-adaptive grids makes it difficult to capture all relevant flow features of unsteady phenomena, as this would require either a high resolution throughout the flow field or a high-quality, manually designed grid. Such a non-adaptive grid would need to be properly fitted to the flow field solution. As the computational solution is not known a-priori and in addition affected by the local grid resolution, the manual design of a grid would usually include several labor-intensive iteration cycles where the grid is adjusted according to the expected and

actual computational solution. In case of unsteady simulations, the refined area needs to capture larger portions of the flow domain which make the grid computationally less efficient. A remedy to this is the use of an adaptive flow solver which automatically detects all flow features and locally adapts the grid during the solution process. To the author's knowledge, Adaptive Mesh Refinement (AMR) has been rarely used in literature to simulate shock-shock interactions employing non-ideal gas assumptions.[70] AMR relies on a gradient-based adaptation of the flow field. However, as shock-shock interactions may be potentially unstable and will not lead to a pronounced convergence behavior, an adaptation solely based on the flow field quantities is a more promising approach. This is why the multiscale-based grid adaptation concept is used in the present work. Locally refined areas in combination with hanging nodes allow to capture all important flow phenomena, without the need to sacrifice the proper resolution in certain areas for the sake of lower computational costs. Grid convergence can be easily addressed by applying another grid adaptation to refine the grid.

Several authors noted the strong dependence of the solution on the grid quality. Systematic studies of the required cell size for the proper resolution of the wall heat flux were carried out by Hoffmann et al.[63] It was found that the required grid size depends on the Mach number and the Reynolds number. Olejniczak et al.[105] investigated inviscid shock-shock interactions on a double ramp and noted the strong sensitivity of the shock angles and contact surfaces to the proper resolution of the triple points.

Unsteady Mechanism The Edney type IV interaction is known as being inherently unstable.[80] Different types of behavior are found in the literature which range from fully unsteady to steady flow characteristics of the jet structure. No comprehensive systematic studies of the unsteady behavior are known to the author. However, the unsteady characteristics of particular configurations are subject to various publications.

Referring to Lind and Lewis,[83] the unsteadiness of the Edney type IV interaction depends strongly on the angle and strength of the oblique shock wave and its impingement location on the bow shock. They observed that small changes in the impinging shock properties may cause steady flow fields to become unsteady. Following their observations,[83] *"the high-frequency jet unsteadiness is seen to be related to the formation of a vortex near the junction of upper shear layer and the termination point of the supersonic jet, its breakdown, and then its propagation along the upper portion of the cylinder, causing shear layers to be generated and then shed."* The shedding frequency was analyzed by means of a Fourier analysis to be in the order of 1.4 kHz for a test case with stronger oscillations from several investigated configurations. This frequency was also confirmed by the variation of the peak pressure at the wall. The published plots of the peak pressure and the jet impingement angle for a particular configuration show a quite regular pattern with only minor variations in the magnitude over a longer period of time. This is in contrast to results of a slightly modified configuration with a lower angle of the oblique shock wave and a higher impingement location on the bow shock.

In this case, only initial oscillations were discovered. These were strongly damped in time and resulted in a steady-state solution. This effect was also supported by a coarser grid resolution. A stronger damping of the oscillations in the initial phase was also observed for an intermediate configuration with a higher angle of the incident shock wave. However, in this case only a solution close to steady-state but with sustained oscillations was reached. All of these ideal gas results were simulated with the TIMETVD code of Yee[83] which is second-order accurate in space and time.

Chu and Lu[29] applied higher-order WENO schemes which are third-order accurate in time to investigate the unsteady behavior of the Edney type IV interaction. The maximum values of the heat flux and the surface pressure were found to show periodic oscillations. A feedback mechanism was proposed as a possible means to investigate the dominant frequency of particular configurations of the shock-shock interaction.

Furumoto et al.[43] also observed the unsteady characteristics of the Edney type IV interaction in their simulations of 5-species air in thermochemical nonequilibrium. The applied numerical code was second-order accurate in space and third-order accurate in time. The investigated configuration resulted in stronger unsteady characteristics in the initial phase of the simulation. A sustained oscillation in the maximum surface pressure could be reached once all transients of the solution were damped out. Furumoto et al. concluded that the most unstable solution was obtained with a shock impingement angle which leads to a shock-shock interaction in the transition regime between a type III and IV interaction. In case of more unstable solutions, *"the largest degree of unsteadiness was the result of alternating shed vortices both above and below the jet"*[43] which is similar to the mechanism described by Lind and Lewis,[83] though the vortex shedding on both sides of the jet seems to be influential in the configuration of Furumoto et al. In a similar study for ideal gases, Zhong[145] identified unsteady characteristics with a frequency in the order of $30\,kHz$.

Yamamoto et al.[143] confirmed the unsteady behavior of the Edney type IV interaction, both for ideal gas and thermochemical nonequilibrium. The applied finite difference scheme was fourth-order in space and second-order in time. Concerning the upwind methods, a modified AUSM scheme was used for ideal gas, whereas the AUSMDV scheme was employed to improve the stability of the simulations in thermochemical nonequilibrium.

Gaitonde[44] simulated an Edney type IV interaction with ideal gas applying a higher-order MUSCL scheme. He observed periodic unsteady behavior with *a large scale movement at a dominant frequency of* $32\,kHz$.

Brück[17] reported an oscillating behavior of the residual in his steady-state simulations of the Edney type IV interaction in thermochemical nonequilibrium which was identified as unsteady behavior. Brück[17] concluded from Furumoto's findings that the influence of the unsteady behavior on the stagnation point quantities is low and only of minor importance. A similar behavior was identified by Kumar[80] in his reactive thermal equilibrium simulations of Sanderson's experiments with an older version of the QUADFLOW solver.

For a low enthalpy case, stronger initial oscillations of the peak Stanton number and the shock impingement angle were observed. The latter approached a steady-state solution, while sustained oscillations with a smaller amplitude were discovered in the peak Stanton number. Kumar[80] concluded that a *"possible reason of the jet unsteadiness could be the propagation of a pressure wave, generated by the interaction between the shock waves in the supersonic jet structure and the shear layer outside the jet, to the upstream direction through the subsonic shock layer"*. Kumar could not identify any vortices, most likely due to the lower resolution of these simulations. Kumar underlined that his observations oppose the earlier investigations by Lind and Lewis[83] and by Furumoto et al.,[43] who identified the previously discussed formation and shedding of vortices as the driving mechanism. However, similar to the investigations of these authors, Kumar found that the unsteady behavior depends strongly on the particular configuration. While a low enthalpy leads to stronger unsteady phenomena, a qualitatively similar, but less pronounced behavior was found for an intermediate enthalpy test case and a high-enthalpy test case. Especially the latter test case was recognized as being close to a steady-state solution. In all of his studies, Kumar applied a local time stepping at the initial stage of the computation to allow for an accelerated convergence. Once all flow features were resolved, a global time stepping allowed a time-accurate unsteady resolution of the flow field.

2.2.3. Test Configuration

Given the above mentioned properties, shock-shock interactions are an excellent application for the QUADFLOW solver. The experimental campaign by Sanderson comprised three shock-shock configurations named cases A to C, as well as a corresponding test series without shock impingement for calibration and validation purposes. Besides these experimental data, computational data by Candler et al.,[20,104] solutions computed with the DLR FLOWer CNE code[78] and solutions computed with an older version of the QUADFLOW solver[121] are available for the flow field without shock impingement. These data serve as a basis on which the validation of the current implementation of the nonequilibrium branch of the QUADFLOW solver can be built. Sanderson's high-enthalpy test case C without shock impingement is selected for the validation and will be discussed in Section 6.1. The medium enthalpy test case B with a freestream temperature of $T_\infty = 1190\,K$ is selected for the simulation of the shock-shock interaction.

In Kumar's[80] simulation of the Edney type IV shock-shock interaction experiment, the former reactive simulations of pure nitrogen were carried out in thermal equilibrium only due to limitations of the older version of the nonequilibrium branch of the QUADFLOW solver. Only two grid adaptations could be used due to the large sensitivity of these simulations to the occurrence of hanging nodes in the boundary layer. Kumar found that this phenomenon was even more severe for the reference simulation without shock impingement. No grid adaptation could be used in this test case. Kumar